Broadband Optical Heterodyne Millimeter-Wave-over-Fiber Wireless Links Based on a Quantum Dash Dual-Wavelength DFB Laser

Khan Zeb, Zhenguo Lu, *Member, IEEE*, Jiaren Liu, Youxin Mao, Guocheng Liu, Philip J. Poole, Mohamed Rahim, Grzegorz Pakulski, Pedro Barrios, Martin Vachon, Daniel Poitras, Weihong Jiang, John Weber, Xiupu Zhang, *Senior Member, IEEE*, and Jianping Yao, *Fellow, IEEE*

***Abstract*—We demonstrate real-time broadband multi-Gb/s electrical RF synthesizer-free millimeter-wave (MMW) signals generation and wireless transmission at the 5G new radio (NR) frequency band of 47 GHz based on analog radio-over-fiber (A-RoF) fronthaul. This is enabled by a low noise, highly correlated, monolithic C-band semiconductor InAs/InP quantum-dash (QDash) dual-wavelength distributed feedback (DW-DFB) laser. One laser mode is encoded using 4-/6-GBaud multilevel quadrature amplitude modulation (M-QAM) (16-/32-/64-QAM) baseband data signals, the other lasing mode is used as an optical local oscillator for optical-heterodyne remote up-conversion to a MMW carrier of 47.27 GHz. Consequently, optical baseband modulated data signals with data capacity up to 36 Gb/s (6-GBaud $\times$ 64-QAM) are transmitted through back-to-back (BtB) and 25-/50-km of standard single mode fiber (SSMF) before the MMW carrier is optically synthesized remotely for free space wireless data transmission and detection over up to 9-m. The end-to-end MMW-over-fiber (MMWoF) wireless link is thoroughly characterized exhibiting promising error-vector-magnitude (EVM) and bit-error-rate (BER) values. The 4-/6-GBaud 16-QAM MMWoF wireless links achieve EVMs down to 6.32%/7.33%, 6.71%/7.78%, and 7.35%/8.91% through BtB, 25-km, and 50-km SSMF, respectively. Similarly, the EVM for 32-QAM and 64-QAM links is observed to be 5.56%/6.56% and 6.05%/6.62%, respectively. Moreover, in each case, the calculated BER is below the forward error correction (FEC) limit of 3.8 $\times$ 10^{-3}. The results corroborate the potential and viability of the QDash DW-DFB laser as a simple, efficient and cost-effective alternative to individual laser sources for deployment in broadband photonic MMWoF fronthaul systems of 5G wireless networks.**

***Index Terms*—5G, broadband wireless communications, fronthaul, microwave photonics, millimeter-wave, optical heterodyning, quantum dash dual-wavelength DFB laser, radio-over-fiber.**

Manuscript received November 18, 2021; revised February 10, 2022; accepted February 17, 2022. Date of publication February 25, 2022; date of current version June 16, 2022. This work was supported in part by the National Research Council Canada's high throughput and secure networks (HTSN) program under Grant HTSN02. *(Corresponding authors: Khan Zeb; Zhenguo Lu)*

Zhenguo Lu, Jiaren Liu, Youxin Mao, Guocheng Liu, Philip J. Poole, Mohamed Rahim, Grzegorz Pakulski, Pedro Barrios, Martin Vachon, Daniel Poitras, Weihong Jiang, and John Weber are with the Advanced Electronics and Photonics Research Center, National Research Council Canada, Ottawa, ON K1A 0R6, Canada (e-mail: zhenguo.lu@nrc-cnrc.gc.ca; jiaren.liu@nrc-cnrc.gc.ca; youxin.mao@nrc-cnrc.gc.ca; guocheng.liu@nrc-cnrc.gc.ca; philip.poole@nrc-cnrc.gc.ca; mohamed.rahim@nrc-cnrc.gc.ca; grzegorz.pakulski@nrc-cnrc.gc.ca; pedro.barrios@nrc-cnrc.gc.ca; martin.vachon@nrc-cnrc.gc.ca; daniel.poitras@nrc-cnrc.gc.ca; weihong.jiang@nrc-cnrc.gc.ca; john.weber@nrc-cnrc.gc.ca).

Khan Zeb is with the Advanced Electronics and Photonics Research Center, National Research Council Canada, Ottawa, ON K1A 0R6, Canada, and also with the iPhotonics Labs, Department of Electrical and Computer Engineering, Concordia University, Montreal, QC H3G 1M8, Canada (e-mail: k_zeb@encs.concordia.ca).

Xiupu Zhang is with the iPhotonics Labs, Department of Electrical and Computer Engineering, Concordia University, Montreal, QC H3G 1M8, Canada (e-mail: johnxiupu.zhang@concordia.ca).

Jianping Yao is with the Microwave Photonics Research Laboratory, School of Electrical Engineering and Computer Science, University of Ottawa, Ottawa, ON K1N 6N5, Canada (e-mail: jpyao@uottawa.ca).

Color versions of one or more figures in this article are available at https://doi.org/10.1109/JLT.2022.3154652.

Digital Object Identifier 10.1109/JLT.2022.3154652

I. Introduction

THE demand for broadband high speed, low latency, reliable and pervasive wireless connectivity has increased manifold since the inception of new technologies and bandwidth hungry applications, such as high definition video streaming, virtual and augmented reality (VR/AR), autonomous vehicles, artificial intelligence, and IoTs [1]–[3]. Furthermore, the Coronavirus crisis has heightened the urgency for broadband connectivity. It has been realized during the pandemic that broadband ubiquitous connectivity matters more than ever before and wireless technology is playing a crucial role. Not only helping people to stay connected around the globe but also enabling telehealth, remote learning and education, and especially remote work that keeps businesses, essential services and government operations running to meet daily needs [4]. This highlights the need and importance of 5G wireless networks, which promise to provide broadband high data rate wireless connectivity with high reliability and low latency pervasively.

The International Telecommunication Union (ITU) specifies 5G standards in International Mobile Telecommunications 2020 (IMT-2020) that identify three different usage scenarios including enhanced mobile broadband (eMBB), massive machine type communication (mMTC) and ultra-reliable low latency communication (URLLC). The eMBB features high speed broadband services with peak data download speed of more than 20-Gb/s and seamless user experience data rates of 100-Mb/s in wider coverage area with the expected speed of Gb/s in hotspot scenarios [5]. These ultra-high speed broadband and low latency services cannot be supported by the already depleted sub-6GHz RF spectrum. Therefore, 5G requires high frequency bands in the millimeter-wave (MMW) spectrum (30 GHz – 300 GHz) with plentiful available bandwidths for the realization of ultra-high speed and high-capacity broadband communications [6]. To this end, 3GPP has standardized higher frequency bands above 24.25 GHz for 5G new radio (NR) designated as frequency range 2 (FR2) (24.25 GHz – 52.6 GHz) [7] and work is underway for frequency bands beyond 52.6 GHz. Nonetheless, the generation and processing of high-speed and broadband MMW signals in an all-electrical setup is hindered by the bandwidth limitation of the electronic devices in addition to cost and complexity. Besides, the transmission of MMW signals over long distances is a real challenge. Consequently, broad bandwidth, simple, efficient, and cost-effective photonic millimeter-wave-over fiber (MMWoF) solutions are considered viable alternatives for MMW signal generation, processing, control and distribution in the optical domain for application in broadband wireless access networks [8], [9]. The optical devices and techniques that are used for MMW signals in conjunction with the bandwidth efficient analog radio-over-fiber (A-RoF) technology not only overcome the problem of high bandwidth requirements, transmission capacity and span limitation but also significantly reduces system complexity [1], [8]–[10], footprint, capital expenditure (CAPEX) and operating expenses (OPEX).

The basic notion of MMW signal generation and distribution in the optical domain through MMWoF links is based on the remote optical heterodyne beating of two phase-correlated optical signals having different wavelengths on a high speed photo detector (PD) after running over several tens of kilometers of optical fiber [11]. Photonic RF signal generation techniques can be used to generate RF signals of up to THz range, limited only by the frequency response of the PD. In this way, seamless fiber-wireless integration can be achieved [12] through generating RF MMW carriers optically, which is inevitable for 5G ultra-broadband wireless networks. Thus, optical heterodyne MMW over A-RoF can significantly simplify the overall fronthaul architecture compare to traditional architecture, especially the RF front end in the centralized cloud radio access network (C-RAN) environment of 5G. This is due to the fact that digital or analog data can be modulated onto either one or two optical signals in the baseband units (BBUs) located in the central office (CO) and the desired RF MMW carrier signal can be remotely synthesized optically right at the antenna eliminating the need for expensive components, such as digital to analog and analog to digital converters (DACs/ADCs) in the case of conventional digital RoF or electrical local oscillators and mixers in the case of conventional A-RoF

However, in the case of the optical heterodyne MMWoF configuration, the phase fluctuations of the two optical signals need to be highly correlated in order to ensure spectrally pure MMW carrier signal generation. Because if the two optical signals are not phase correlated, for instance in the case of two different free running lasers, then the resulting MMW signal ends up with high phase noise thus limiting the system performance [1], [13]. Conversely, if the phase noise of the two optical signals is correlated then the common noise of the two signals cancels out and a low phase noise MMW signal is generated. This entails either the elimination or correlation of phase noise of the corresponding optical signals for the generation of spectrally pure and phase stable MMW carrier signals. Thus highly correlated and integrated optical sources are desirable for 5G MMWoF systems.

Several techniques and devices have been proposed and demonstrated for optical heterodyne MMW signal generation and data transmission in RoF links based on schemes such as using two individual single wavelength lasers [2], external modulation of a single mode laser [14]–[16], picking pairs of modes from optical frequency combs [13], [17], [18], sources based on colorless laser diode [19]–[22] and dual-wavelength optical sources [23], [24]. Similarly, several techniques have been reported for the phase locking and stabilization between the two optical heterodyne signals including optical injection locking [25], [26], optical-phase-locked-loop (OPLL) [27] and their combination [28].

These MMW sources and stabilization techniques offer better frequency correlation and stabilization than any two free-running lasers based schemes. Nevertheless, most of the MMW signal generation techniques utilizing phase locking and stabilization approaches rely on complex and expensive devices, such as modulators, microwave reference sources and other related components that add to the complexity and cost of the transmitter system. In addition, the bias drift associated with some of the aforementioned schemes involving external modulators can cause instability, hence limiting system performance. Consequently, besides attaining spectral purity and stability, the complexity and cost are the two key factors that need to be considered in the design of future 5G wireless systems

In recent years, semiconductor quantum dash (QDash) multi-wavelength lasers have gathered considerable attention for photonic MMW signal generation and applications in optical heterodyne MMWoF systems [1], [3], [29]–[41]. Compared with other technologies well-designed quantum confined nanostructures, such as semiconductor InAs/InP QDash lasers, have the distinctive advantage of achieving highly coherent and correlated optical signals with very low phase and intensity noise [29], [33], [38], [42]–[44], together with chip-scale integration viability. Moreover, for further spectral purity and phase stabilization in such highly integrated and correlated devices, a simple feedback mechanism of self-injection locking can be used [1], [30], [42], [45], [46] eliminating the need for comparatively more complex and expensive components, thus making them a suitable candidate as an optical MMW source for 5G MMWoF systems.

A number of InP based QDash multi-wavelength lasers are demonstrated as optical MMW sources in both C-band [1], [3], [29], [30], [33]–[35], [37]–[41] and L-band [31], [32], [35], [41]. These include some recent experimental demonstration of optical heterodyne MMWoF links using QDash passively mode-locked lasers (MLLs) or optical frequency combs [1], [29], [30], [37] in the C-band, QDash injection-locked laser diodes in the C-band [34], [35], [39]– [41] and L-band [31], [32], [36], [41], and two wavelengths in a free running state from a monolithically integrated QDash Y-coupled dual-DFB lasers source [38] and a QDash common-cavity dual-wavelength DFB

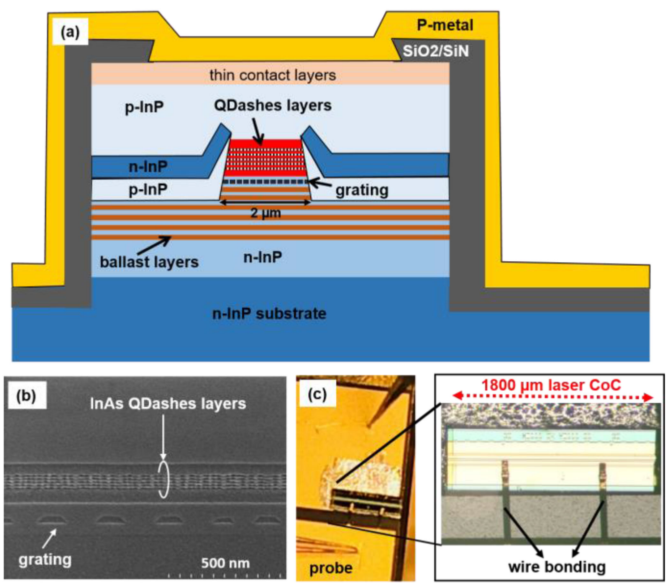

Fig. 1. (a) Schematic of the cross-section of the QDash DW-DFB laser (b) SEM image of the lateral cross-section through the middle of the mesa of the device showing synthesized aperiodic grating underneath 5 stack layers of QDashes (c) QDash DW-DFB laser CoC.

(DW-DFB) laser in the C-band [3]. Compared with other optical sources, such as QDash combs or QDash injection locked laser diodes and dual-mode devices based on separate DFB cavities or individual DFB lasers, QDash common-cavity DW-DFB laser offers a compact and simple solution for MMWoF systems by generating two different wavelengths from within the same cavity featuring high output optical power and low noise [33]. This results in high optical power per mode (significantly higher than for a QDash comb laser) and high spectral purity with low phase and relative intensity noise. Importantly, this makes the device comparatively simple and compact. Consequently, the QDash dual-wavelength DFB laser has the advantage of reducing system complexity and cost showing the potential to offer a simple and low cost solution for 5G optical heterodyne MMWoF systems.

In this paper, we extend our work on the use of an InAs/InP QDash DW-DFB laser in [3] for MMWoF systems with the experimental demonstration of broadband multi-Gb/s optical heterodyne MMWoF wireless links at 5G NR frequency of around 47.27 GHz. The demonstration includes electrical RF synthesizer-free real-time photonic generation, wireless transmission and detection of wide-bandwidth MMW M-QAM modulated (16-QAM, 32-QAM and 64-QAM) data signals having symbol rate of 4- and 6-GHz with bit rates ranging from 16 Gb/s (4-GBaud $\times$ 16-QAM) to 36 Gb/s (6-GBaud $\times$ 64-QAM) over hybrid fiber-wireless links comprising of back-to-back (BtB), 25-km and 50-km SSMF and 2-m to 9-m free-space wireless channel. After long-reach transmission of baseband data modulated optical signal in 25-/50-km SSMF, the MMW carrier is optically-synthesized remotely through optical-heterodyning for free space wireless data transmission. This ensures the transmission and distribution of ultra-high frequency MMW signals over long distances with better performance. Moreover, a thorough end-to-end optical-MMW link analysis is performed with different M-QAM, fiber spans, MMW link distances and data transmission bandwidths to evaluate the transmission performance of the proposed QDash DW-DFB laser based MMWoF system in terms of EVM, BER, constellations and eye diagrams. To the best of our knowledge, this is the first experimental demonstration to realize MMWoF wireless links at the potential 5G NR frequency band of around 47.27 GHz with real-time wireless transmission and detection of wideband MMW M-QAM (16-/32-/64-QAM) modulated data signals having a maximum bit rate of 36 Gb/s using a free-running InAs/InP QDash DW-DFB laser. The generated MMW frequency range from 46 GHz to 48 GHz of the device falls within the potential 3GPP 5G NR standard band (n262) of frequency range 2 (FR2) offering a promising optical MMW source for 5G MMWoF systems.

The remainder of this paper is organized as follows. Section II presents a brief description of the design, implementation and characterization of the QDash DW-DFB laser. Section III presents the proposed QDash DW-DFB laser based MMWoF wireless system design and detailed implementation. It is followed by the experimental results and discussion in Section IV. Finally, section V presents the conclusion.

II. Quantum Dash Dual-Wavelength DFB Laser

The laser source used in this study is an InP based p-n-blocked buried heterostructure common cavity dual-mode QDash DFB laser. Fig. 1(a) shows a schematic of the cross-section of the laser. The gain region of the device consists of 5 layers of InAs QDashes in a 170 nm thick InGaAsP waveguiding core with 10 nm $In_{0.816}Ga_{0.184}As_{0.392}P_{0.608}$ (1.15Q) barriers. This active region is surrounded by n-type and p-type InP cladding layers as shown in Fig. 1(a). In the lower n-type InP cladding, 1.03Q ballast layers are employed to pull the mode into the n-type region, which helps in reducing cavity loss and increase efficiency. This also reduces the spontaneous emission coupling to the optical mode. The InAs QDash material was grown on (001)-oriented n-type InP substrate using chemical beam epitaxy (CBE) [47] followed by further etch and regrowth steps using metal-organic chemical vapor deposition (MOCVD) to create buried the heterostructure. The 1800 µm long laser waveguide was fabricated through standard photolithograph with dry- and wet-etching and contact metallization techniques.

An e-beam written novel synthesized aperiodic non-uniform diffraction grating is incorporated below the QDash active layers in the n-type InP cladding as shown in Fig. 1(a). This can also be seen in the scanning electron microscope (SEM) image of the lateral cross-section of the device below the 5 stack layers of QDashes in Fig. 1(b). This generates two highly correlated longitudinal modes simultaneously at different wavelengths with a drive current and temperature controlled tunable MMW frequency range between 46 and 48 GHz from within the single optical cavity of the device with QDash active layers. A full description of the grating can be found in [33]. After the growth of the laser core, a 2 µm wide mesa is formed by etching through the 1.15Q waveguide core and grating layer using dielectric mask followed by selective area overgrowth of pnp blocking

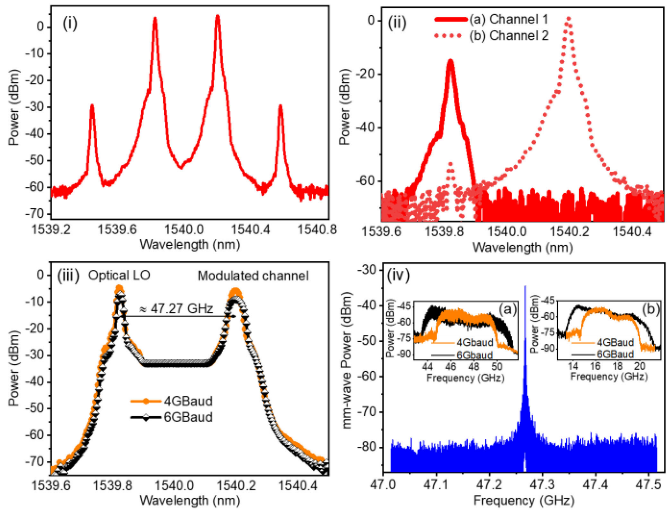

Fig. 2. Measured (i) optical spectrum of the QDash DW-DFB laser at the BBU after isolator (ii) optical spectrum of (a) channel 1 (optical LO) and (b) channel 2 (data channel) after TOBPF1 and TOBPF2, respectively, (iii) unmodulated (optical LO) and optical modulated data channel at the PD, and (iv) typical spectrum of the MMW carrier at the UE before down-conversion with insets showing the received 4-GBaud and 6-GBaud modulated 16-QAM data signals occupying 5.4 GHz and 8.1 GHz transmission bandwidth, respectively (a) before mixer and (b) after mixer by down-converting to IF.

layers to confine the carriers to the waveguide mesa. Finally the dielectric mask was removed and p-type InP cladding and contact layers were grown. After cleaving both facets of the device were AR coated.

The 1800 μm long laser chip is mounted on a commercially available Aluminium Nitride (AlN) carrier to provide mechanical support to the device. The chip on carrier (CoC) is shown in Fig. 1(c). The QDash laser chip is bonded to the carrier with Gold Tin (AuSn) providing the cathode connection, with the top contact being wire bonded for the anode connection as shown in Fig. 1(c). The laser threshold current is around 70 mA and the device can provide up to 50 mW average output power at higher injection current.

The output optical spectrum of the laser is comprised of two dominant optical modes with equal amplitudes at two different wavelengths (1539.821 nm and 1540.195 nm) around 0.374 nm apart as shown in Fig. 2(i). Generating both frequencies in the same cavity significantly reduces noise and linewidth of the generated light. Two four wave mixing (FWM) modes can also be seen in the spectrum that originate from the self-mixing of the two primary optical modes within the laser cavity [33]. This shows nonlinear effects of the cavity, which is believed to result in phase locking of the modes, hence reducing their relative amplitude and phase variation. This further stabilizes modal amplitudes and relative phase of the QDash DW-DFB laser. The integrated relative intensity noise (RIN) and optical linewidth for each individual channel are measured to be typically less than −150 dB/Hz in the frequency range from 10 MHz to 20 GHz and 30 kHz with the lowest recorded down to −158.3 dB/Hz and 15.83 kHz, respectively, in free running operation. This subsequently results in generating a low phase noise optical heterodyne MMW carrier beat signal with a 3-dB linewidth of typically 40 kHz or narrower [3], [33].

Note that by changing drive current and temperature the mode spacing can be tuned by around 0.0158 nm, which corresponds to tuning MMW frequency range from 46 GHz to 48 GHz. However, the RF beat note of the QDash DW-DFB laser can be adjusted from the GHz to the THz range by modifying the design of the synthesized aperiodic grating of the device for the desired spectrum.

III. Design and Experimental Configuration of QDash DW-DFB Laser Based Optical Heterodyne MMWoF Wireless System

A schematic of the experimental configuration for the proposed optical heterodyne MMWoF wireless system is depicted in Fig. 3. In our demonstration, we emulate a typical 5G C-RAN fronthaul architecture where the experimental setup is comprised of a baseband unit (BBU) connected to an RF electrical LO-free optical heterodyne synthesizer based remote radio unit (RRU) through a 25-km or 50-km SSMF link followed by 2-m to 9-m MMW free space indoor RF wireless link connecting to the MMW user equipment (EU). Fig. 4 shows a detailed component pictorial view of the experimental setup including the MMWoF wireless transmission link. In the BBU, the InAs/InP QDash common cavity DW-DFB laser is employed as the main optical source. In our experiments the CoC is placed on a copper block with a thermoelectric cooler (TEC) underneath for temperature control. The temperature of the CoC and the laser bias current are controlled through a laser diode controller (ILX Lightwave, Model LDC-3722) where the laser is biased through a pair of DC electrical probes as shown in Fig. 3 and the inset of Fig. 4. Throughout our experiments, the temperature and injection current of the CoC are maintained at 18°C and 360 mA, respectively.

In the BBU, the laser output power is coupled from its front facet through a lensed single mode polarization maintaining fiber (SMPMF) followed by a two stage PM isolator to avoid back reflection into the laser cavity. The light is then split into two paths by employing a 10/90 PM optical coupler (OC_1) followed by two tunable optical band pass filters (TOBPFs). The two optical filters, $TOBPF_1$ and $TOBPF_2$, separate the two optical modes having a frequency spacing of around 47.27 GHz into channel 1 (1539.821 nm) and channel 2 (1540.195 nm) as shown in Fig. 2 (ii). Channel 2 is used as the optical modulated channel for long-reach data transmission whereas channel 1 is used as an un-modulated optical LO for remote optical heterodyning to optically synthesize the MMW carrier for free space wireless data transmission.

As a proof of concept, a QAM optical transmitter having thermally stable in-phase/quadrature (I/Q) Lithium Niobate ($LiNbO_3$) Mach-Zehnder modulator (MZM) and linear data driver electrical amplifiers (EAs) is used in our experiments to realize the data modulated optical channel. Consequently, channel 2 is modulated with baseband 16-, 32-, and 64-QAM data signals having symbol rate of 4-GHz and 6-GHz that are

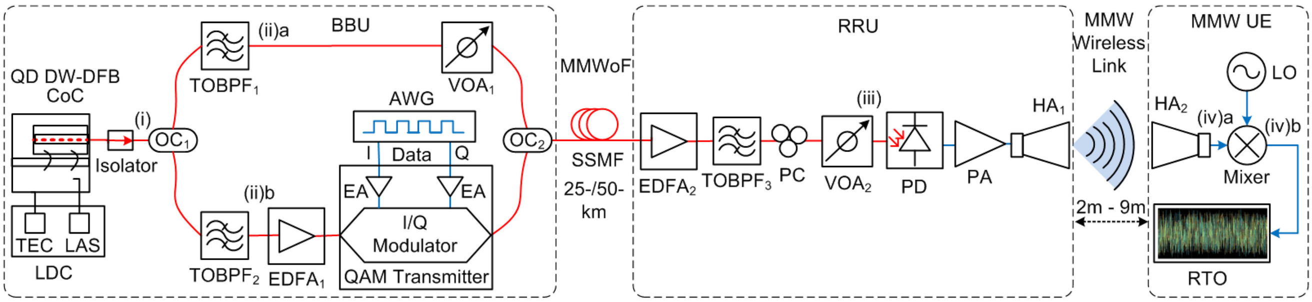

Fig. 3. Schematic of the system experimental setup for the optical heterodyne MMWoF wireless links based on the QDash DW-DFB laser. BBU: baseband unit; RRU: remote antenna unit: MMW UE: millimeter-wave user equipment; CoC: chip-on carrier; OC: optical coupler; TEC: thermoelectric cooler; LAS: laser; LDC: laser diode controller; TOBPF: tunable optical band pass filter; EDFA: erbium doped fiber amplifier; AWG: arbitrary waveform generator; EA: electrical amplifier; VOA: variable optical attenuator; PC: polarization controller; PA: power amplifier; HA: horn antenna; LO: local oscillator; RTO: real-time oscilloscope.

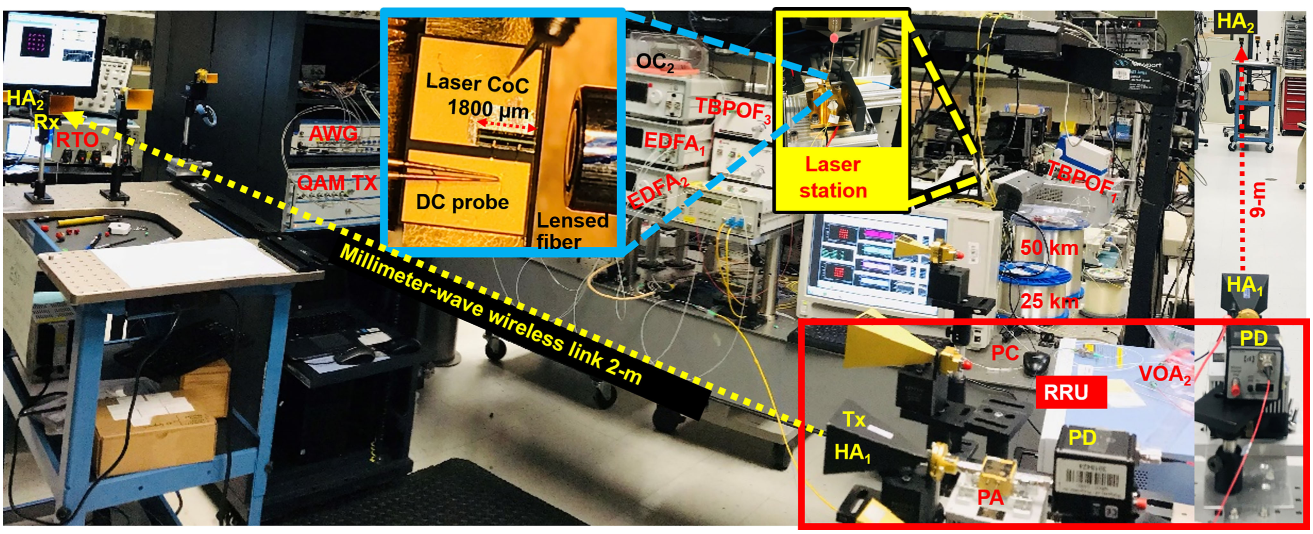

Fig. 4. Photos of the Laboratory experimental setup of QDash DW-DFB laser based optical heterodyne MMWoF system with insets showing the QDash DW-DFB laser CoC on a laser testing station, MMW wireless transmission links (2-m to 9-m), SSMFs (25 & 50-km), wireless transmitter (Tx) and receiver (Rx) and all the other key components of BBU, RRU and MMW UE.

generated electronically by a 65-GSa/s arbitrary waveform generator (AWG) (Keysight M8195A) with a pseudo-random binary sequence (PRBS) pattern of $2^{11}-1$ bits where the bit sequence is mapped onto the I and Q components of the signals. The corresponding data signals are then passed through a root raised cosine (RRC) filter with a roll-off factor of 0.35 for Nyquist pulse shaping. After pulse shaping, the signals are resampled and channel corrections are applied for amplitude flatness before feeding them to the optical transmitter. The data signals are then amplified by two linear data EAs in the optical transmitter before they are fed to I/Q MZM for modulation. Before modulation, the data channel is boosted with an erbium-doped fiber amplifier ($EDFA_1$) to compensate for the insertion loss of the filter and optical modulation transmitter. A PM variable optical attenuator (VOA_1) is also employed in the un-modulated path to equalize its power level to that of modulated channel since the two paths have different losses.

The effective path length difference between the two arms of the transmitter can affect the degree of phase correlation between the two wavelength signals, potentially leading to relatively high phase noise in the generated mm-wave carrier [1], [13]. This decorrelation between the two channels can be avoided by incorporating an optical delay line in the unmodulated path to equalize the effective path lengths. In this way the QAM modulated 47.27 MMW carrier signal is realized in the optical domain with a maximum data rate of 36 Gb/s. Finally, the modulated and unmodulated optical channels are combined in a 50/50 OC_2 and transmitted over the optical fiber link to the RRU. The optical fiber link is comprised of 25-km or 50-km SSMF spool as highlighted in Fig. 4.

The received optical signal at the RRU is amplified through $EDFA_2$ followed by $OBPF_3$ to remove the amplified spontaneous emission (ASE) noise as shown in Fig. 3 and Fig. 4. The optical spectrum of the corresponding received modulated and un-modulated carriers before the PD is shown in Fig. 2 (iii). The photo-mixing output of these two optical frequency signals on a high speed PD (Newport Model-1014), is directly attached to a 22-24 dBi Horn antenna (HA_1) (WR-22) through an RF Q-band power amplifier (PA) with a nominal gain of 45 dB. Thus, a MMW carrier of around 47.27 GHz is optically synthesized remotely without using any electrical LO and the optical data is translated to the corresponding MMW carrier. The data signal on the 47.27 GHz MMW carrier is subsequently transmitted over the 2-m to 9-m wireless link. A polarization controller (PC) is incorporated in the RRU to adjust the polarization direction of the incoming optical signal before photo-mixing to ensure maximum output power at the output of PD. A PM VOA_2 is also employed at the RRU before the PD to control the received incident power on the PD for different wireless link measurements. Note that similar to the transmitter system at the BBU, we use off-the-shelf components at the RRU to demonstrate our proof-of-concept broadband multi-Gb/s MMWoF system. Nevertheless, all of these components, where the EDFAs can be replaced by semiconductor optical amplifiers (SOAs), could be heterogeneously integrated to microwave photonic circuits making the BBU and the RRU more simple compared with the conventional RoF fronthaul systems.

The MMW data signal is received by another identical Horn antenna at the user equipment (UE) over the free space wireless link. This MMW signal is then down-converted to an intermediate frequency (IF) of around 17.3 GHz with an electrical LO before capturing into a real-time oscilloscope (RTO) for processing as shown in Fig. 3. Fig. 2 (iv) shows the corresponding received MMW carrier of 47.27 GHz along with the 4-GBaud and 6-GBaud modulated 16 QAM data signals in the insets (a) before and (b) after down-conversion, occupying transmission bandwidth of 5.4 GHz and 8.1 GHz, respectively. After down-converting the received MMW signal to an IF, as shown in the inset (b) of Fig. 2 (iv), it is coherently detected and processed in real-time by employing vector signal analysis software (SignalVu) on a 100 GSa/s Tektronix DPO73304SX oscilloscope having 33-GHz analog bandwidth. The signal undergoes several digital signal processing (DSP) steps including resampling, clock recovery, digital down-conversion, match filtering, synchronization, and adaptive equalization before it is demodulated to measure the error vector magnitude (EVM) and calculate the bit error rate (BER). For match filtering, an RRC matched filter with roll-off factor of 0.35 is employed to recover the baseband IQ data and to minimize inter-symbol interference (ISI). Similarly, a decision-directed, feed-forward (FIR) adaptive equalizer is used to compensate for linear distortions. Finally, the system integrity and communication performance is evaluated in terms of measured EVM and calculated BER [48].

IV. Experimental Results and Discussion

The performance of the whole MMWoF wireless system is thoroughly analyzed in terms of EVM, BER, constellations, and eye diagrams. Multilevel QAM signals including 16-QAM, 32-QAM and 64-QAM are used to realize MMW wireless links with link capacities ranging from 16-Gb/s to 36-Gb/s. The system performance is then evaluated for different line rates over a fixed MMW wireless link through different fiber lengths by varying the received optical power (ROP), and for different wireless link lengths by changing the wireless transmission distance at a fixed ROP through a 25 km SSMF.

Fig. 5(a) and (b) summarize the EVM performance results of 4-GBaud and 6-GBaud 16-QAM signals with data rates of 16 Gb/s and 24 Gb/s, respectively, over a 2-m MMW wireless link

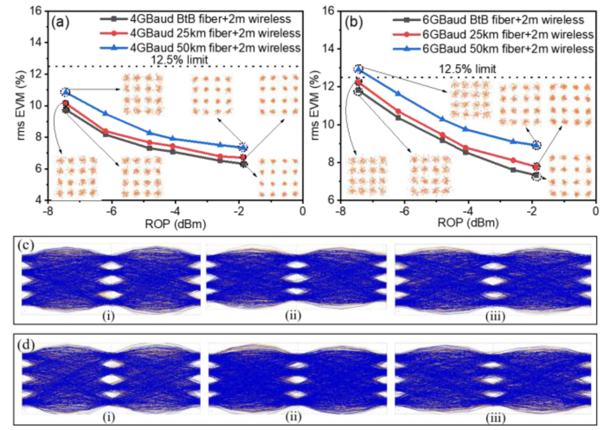

Fig. 5. rms EVM measured at the UE versus ROP at the PD for 16-QAM modulated data signals with (a) 4-GBaud symbol rate occupying 5.4 GHz bandwidth and (b) 6-GBaud symbol rate occupying 8.1 GHz bandwidth. Eye diagrams recorded at the UE over 2-m wireless link at the ROP of ~ -1.9 dBm for 16-QAM (c) 4-GBaud and (d) 6-GBaud through (i) BtB, (ii) 25-km, and (iii) 50-km SSMF link, respectively.

through BtB, 25-km and 50 km SSMF. The different fiber lengths and signal bandwidths are employed to analyze and compare the fiber and signal bandwidth induced impact on the performance with BtB as a reference. In each case, the root mean square (rms) EVM of the 4-GBaud and 6-GBaud 16-QAM wirelessly received MMW signals is measured in real-time at the MMW UE shown in Fig. 3 for different ROPs at the PD. Note that in order to analyze the effect of the optical fiber transmission on the wireless link, the ROP for all of the three fiber lengths is kept identical at the PD by using VAO_2 as shown in Fig. 3.

The results show that for all 16-QAM signals, the EVM is below the 3GPP standard requirement of 12.5%, except for the case of 6-GBaud transmission through a SSMF length of 50 km, where it is slightly over the limit at the ROP of around -7.5 dBm. The inset of Fig. 5(a) and (b) also include clear constellation diagrams showing the successful detection of the corresponding 4-GBaud and 6-GBaud 16-QAM MMW signals at the ROP of -1.9 dBm and -7.5 dBm, respectively. This is also evident from the open eye diagrams of the corresponding wirelessly received 4-GBaud and 6-GBaud 16-QAM signals as depicted in Fig. 5(c) and (d), respectively, at the ROP of -1.9 dBm for the (i) BtB, (ii) 25 km, and (iii) 50 km scenarios. Moreover, Fig. 6 depicts the rms EVM as function of the baud rate for the successful detection of 16-QAM modulated optical heterodyne MMW signals, centered at around 47.27 GHz, over 2-m wireless link through BtB, 25-km and 50-km SSMF at the ROP of -1.9 dBm.

Fig. 7 plots the calculated BER versus the ROP for both 4-GBaud and 6-GBaud 16-QAM MMW signals through BtB, 25 km and 50 km SSMF. The BER is calculated based on the measured rms EVM using the relationship between EVM and BER derived in [48]. It is noted that the BER increases with the increase in baud rate from 4-GBaud to 6-GBaud at the same ROP. A BER $< 10^{-9}$ is observed for 4-GBaud transmissions at the ROP of > -2.5 dBm for all of the three scenarios. However, for 6-GBaud transmissions, the same is only observed in the case of BtB scenario as shown in Fig. 7. Overall, the

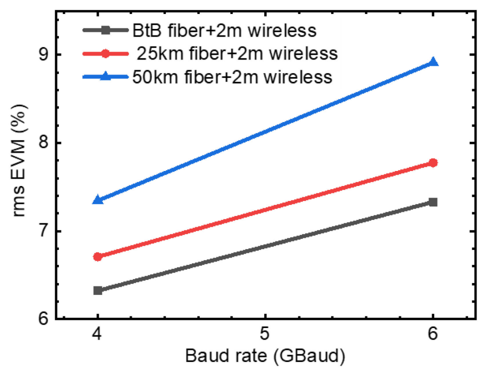

Fig. 6. rms EVM as a function of the baud rate for 16-QAM MMWoF wireless links at the ROP of ∼ −1.9 dBm .

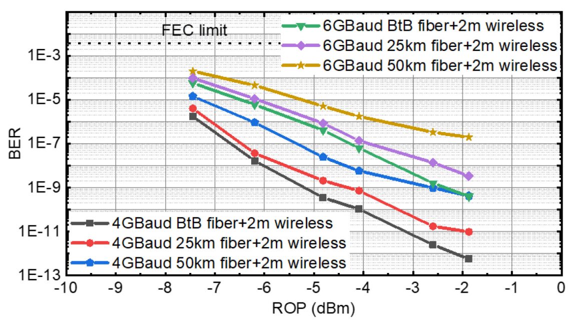

Fig. 7. Calculated BER as a function of ROP for 4-GBaud and 6-GBaud 16-QAM data signals measured over 2-m MMW wireless link through BtB, 25-km and 50-km SSMF.

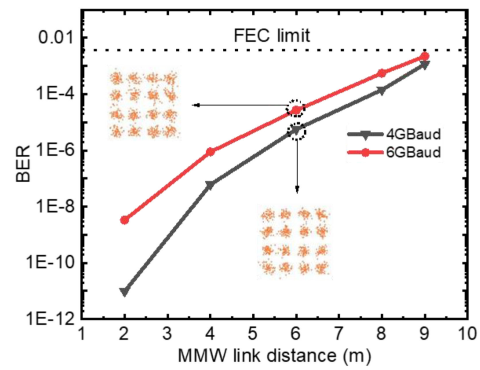

Fig. 8. BER versus MMW wireless link distance at ROP of ∼ −1.9 dBm for 4-GBaud and 6-GBaud 16-QAM received signals through 25-km SSMF.

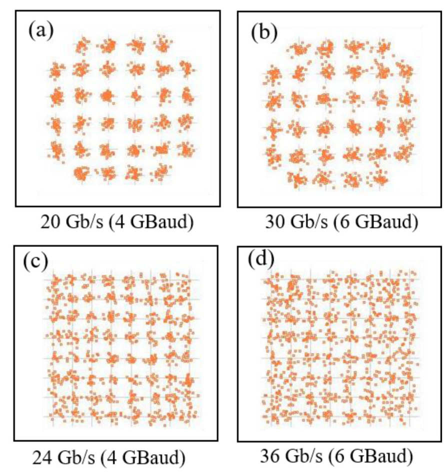

Fig. 9. Wirelessly received signal constellations of (a) 4-GBaud 32-QAM (20 Gb/s), (b) 6-GBaud 32-QAM (30 Gb/s), (c) 4-GBaud 64-QAM (24 Gb/s), and (d) 6-GBaud 64-QAM (36 Gb/s).

BER performance for both 4-GBaud and 6-GBaud transmissions under all scenarios is below the standard FEC limit of 3.8×10^{-3}.

Generally, an increase in performance degradation is observed with an increase in bandwidth of the transmitted signals from 5.4 GHz to 8.1 GHz having baud rate of 4-GBaud and 6-GBaud, respectively, as can be seen from Fig. 6. This is attributed to the fact that the MMWoF system is more prone to noise and propagation loss at wideband signal operation. However, it is observed that on average, the fiber length of 25 km induces slight performance degradation with EVM penalty of around 0.4 dB for both 4-GBaud and 6-GBaud optical heterodyne MMW wireless transmissions with respect to their BtB scenarios. This degradation further increases to around 1.1 dB and 1.2 dB for 4-GBaud and 6-GBaud transmissions, respectively, in the case of 50-km fiber. Similarly, an average penalty of around 0.7 dB and 0.8 dB is observed between 25-km and 50-km transmissions of 4-GBaud and 6-GBaud mm-wave signals, respectively. Nevertheless, an average degradation of about 1.7 dB is observed between the transmissions of 4-GBaud and 6-GBaud 16-QAM MMW signals through BtB, 25-km and 50-km SSMF, which corresponds to an average optical power penalty of around 2.8 dB. This is ascribed to the very nature of the wide bandwidth operation encountering relatively more noise, fiber dispersion and channel propagation loss at the MMW frequency. A typical spectrum of the received modulated MMW data signals at the UE with 5.4 GHz and 8.1 GHz transmission bandwidths both before and after down-conversion can be seen in the inset (a) and (b) of Fig. 2 (iv), respectively, for the ROP of around −1.9 dBm at the PD. The uneven envelop of the received modulated signals towards the high frequency end is due to the operating frequency range of the PD, PA and antennas.

Thus, the EVM and BER performance degradation with fiber length in the aforementioned cases is believed to be due to the accumulated dispersion encountered over the optical fiber link along with the effective path length difference between the two optical carriers at the transmitter [1] and the corresponding wireless propagation path loss. To further improve the results, an optical delay line can be incorporated in the un-modulated path at the transmitter side and dispersion compensation can be employed to further reduce the effect of optical carrier decorrelation at the PD [13]. Besides, it is observed that polarization misalignment impacts the results, which can be avoided by employing proper polarization control. In addition, based on the antennas configuration in our experiments, accurate direct line-of-sight (LOS) path is required from the transmitter antenna to the receiver antenna to establish a link with better performance.

The effect of the MMW wireless link length on the performance of the system is also investigated. Fig. 8 shows the BER performance at different wireless link distances through a 25-km SSMF at a fixed ROP of around −1.9 dBm for both

4-GBaud and 6-GBaud 16-QAM signals. Their corresponding constellation diagrams for a wireless link distance of 6-m are also shown in Fig. 8. The measured EVM values for these constellation diagrams of 4-Gbaud and 6-Gbaud received signals were 10.33% and 11.26% respectively. The results show that BER performance of under the FEC limit of 3.8×10^{-3} is achieved for both 4- and 6-GBaud MMW signals wireless transmissions with a maximum MMW link distance of 9-m at the ROP of -1.9 dBm. It is apparent that the 4-GBaud 16-QAM signal achieves better BER performance as compared to 6-GBaud 16-QAM. However, in both cases, the performance deteriorates as the wireless distance increases. In general, it is observed that increase in the RF link distance or decrease in the ROP degrades the system performance. This is attributed to the wireless propagation path loss along with imprecise antenna alignment and increase in noise level at the received low MMW signal power that results in low electrical signal to noise ratio (ESNR) contributing to the performance degradation. Moreover, since we use directional antennas in our experiments their alignment becomes critical as the wireless distance increases and the lack of proper LOS impacts the link performance.

Finally, Fig. 9(a) and (b) and Fig. 9(c) and (d) show the constellation diagrams for 4- and 6-GBaud 32-QAM and 64-QAM MMWoF wireless links, respectively, with 25-km SSMF and 2-m wireless distance at the ROP of around -1.9 dBm at the PD. The rms EVM values for 4-/6-Gbaud 32-QAM and 64-QAM links with a transmission bandwidth of 5.4-/8.1-GHz were measured to be 5.56%/6.56% and 6.05%/6.62%, respectively. Fig. 9(a) and (b) show the comparison between 4-GBaud and 6-GBaud 32-QAM MMW signals transmissions with the calculated BERs of 7.26×10^{-9} and 7.06×10^{-7}, respectively. Similarly, Fig. 9(c) and (d) show the comparison between the MMWoF wireless transmission of 4-GBaud and 6-GBaud 64-QAM MMW signals with the calculated BER of 8.94×10^{-5} and 2.84×10^{-4}, respectively. This constitutes a link data throughput of 20 Gb/s and 30 Gb/s in the case of 4- and 6-GBaud 32-QAM signals, and 24 Gb/s and 36 Gb/s in the case 64-QAM signals, respectively.

The results show that the QDash DW-DFB laser based optical heterodyne MMWoF wireless links achieve EVM and BER performance of under the FEC limit in all cases for both 4- and 6-GBaud wideband 47.27 GHz MMW wireless signals transmissions with a minimum BER of 5.7×10^{-13} and 4×10^{-10}, respectively, and a maximum bit rate of 36 Gb/s. These results demonstrate the capabilities of QDash DW-DFB lasers with the MMW frequency range within the 5G NR standard band (n262) of FR2 as a promising optical MMW source for 5G optical heterodyne synthesizer based MMWoF wireless systems.

V. Conclusion

We successfully demonstrate various real-time broadband optical heterodyne synthesizer based MMWoF wireless links featuring multi-Gb/s data rates with a maximum data capacity of 36 Gb/s (64-QAM $\times$ 6-GBaud) having EVM and BER below the standard 7% overhead FEC limit of 3.8×10^{-3} using a free running QDash DW-DFB laser. The results indicate that the optical heterodyning of two highly correlated and low noise optical signals is an efficient method for transporting and distributing high frequency MMW data signals in the optical domain over long distances. After long-reach transmission of these basebands data modulated optical signals, the corresponding desired MMW modulated carrier signal can be optically-synthesized remotely through photonic up-conversion in the MMW RoF systems for free space wireless data transmission. This greatly simplifies the overall system by preserving any modulated data format on the optical signals and translating it to the corresponding MMW carrier signal. This eliminates front end expensive components, such as electrical LOs and ADCs/DACs at the RRU. This highlights the potential of low noise, correlated and monolithically integrated InAs/InP QDash DW-DFB lasers for deployment as an alternative to individual DFB lasers in 5G optical heterodyne MMWoF systems.

References

[1] A. Delmade *et al.*, "Optical heterodyne analog radio-over-fiber link for millimeter-wave wireless systems," *J. Light. Technol.*, vol. 39, no. 2, pp. 465–474, Jan. 2021.

[2] X. Li *et al.*, "1-Tb/s millimeter-wave signal wireless delivery at D-band," *J. Light. Technol.*, vol. 37, no. 1, pp. 196–204, Jan. 2019.

[3] K. Zeb *et al.*, "A quantum-dash dual-wavelength DFB laser for optical millimeter-wave radio-over-fiber systems," in *Proc. Opt. Fiber Commun. Conf.*, 2021, pp. 1–3.

[4] C. Amon, "How mission critical connectivity has helped the world adapt to COVID-19–and prepare for the next crisis," on the agenda of World Economic Forum, Accessed: Apr. 2020. [Online] Available: https://www.weforum.org/agenda/2020/04/how-mission-critical-connectivity-has-helped-the-world-adapt-to-covid-19-and-prepare-for-the-next-crisis/

[5] M. Series, "IMT Vision—Framework and overall objectives of the future development of imt for 2020 and beyond," Series of ITU-R Recommendations, Rec. ITU-R M.2083-0, Sep. 2015. [Online]. Available: https://www.itu.int/rec/R-REC-M.2083-0-201509-I/en

[6] H. -Y. Wang, C. -H. Cheng, B. Su, and G. -R. Lin, "QAM-GFDM of dual-mode VCSEL mixed 28-GHz MMW carrier for fiber-wireless link," *J. Lightw. Technol.*, vol. 39, no. 19, pp. 6076–6084, Oct. 2021, doi: 10.1109/JLT.2021.3096246.

[7] 3rd Generation. Partnership Project (3GPP), "User equipment (UE) radio transmission and reception; Part 2: Range 2 standalone (Release 15)," 3GPP, Tech. Spec. 38.101-2, V15.1.0, 2018. [Online]. Available: https://www.3gpp.org/ftp//Specs/archive/38_series/38.101-2/38101-2-f10.zip

[8] J. Yao, "Microwave photonics," *J. Light. Technol.*, vol. 27, no. 3, pp. 314–335, Feb. 2009.

[9] J. Yu, "Photonics-assisted millimeter-wave wireless communication," *IEEE J. Quantum Electron.*, vol. 53, no. 6, pp. 1–17, Dec. 2017.

[10] C. Lim and A. Nirmalathas, "Radio-over-fiber technology: Present and future," *J. Lightw. Technol.*, vol. 39, no. 4, pp. 881–888, Feb. 2021.

[11] U. Gliese, T. N. Nielsen, S. Nørskov, and K. E. Stubkjaer, "Multifunctional fiber-optic microwave links based on remote heterodyne detection," *IEEE Trans. Microw. Theory Techn.*, vol. 46, no. 5, pp. 458–468, May 1998.

[12] J. Yu, X. Li, and W. Zhou, "Tutorial: Broadband fiber-wireless integration for 5G+ communication," *APL Photon*, vol. 3, no. 11, pp. 111101–1–111101–20, Sep. 2018.

[13] C. Browning *et al.*, "Gain-switched optical frequency combs for future mobile radio-over-fiber millimeter-wave systems," *J. Lightw. Technol.*, vol. 36, no. 19, pp. 4602–4610, Oct. 2018.

[14] J. L. Li, F. Zhao, and J. Yu, "D-band millimeter wave generation and transmission though radio-over-fiber system," *IEEE Photon. J*, vol. 12, no. 2, pp. 1–8, Apr. 2020.

[15] X. Pan *et al.*, "Photonic vector mm-wave signal generation by optical dual-SSB modulation and a single push-pull MZM," *Opt. Lett.*, vol. 44, no. 14, pp. 3570–3573, Jul. 2019.

[16] K. Mallick, P. Mandal, G. C. Mandal, R. Mukherjee, B. Das, and A. S. Patra, "Hybrid MMW-over fiber/OFDM-FSO transmission system based on doublet lens scheme and POLMUX technique," *Opt. Fiber Technol.*, vol. 52, Nov. 2019, Art. no. 101942.

[17] G. K. M. Hasanuzzaman, H. Shams, C. C. Renaud, J. Mitchell, A. J. Seeds, and S. Iezekiel, "Tunable THz signal generation and radio-over-fiber link

based on an optoelectronic oscillator-driven optical frequency comb," *J. Lightw. Technol.*, vol. 38, no. 19, pp. 5240–5247, Oct. 2020.

[18] G. K. M. Hasanuzzaman, A. Kanno, P. T. Dat, and S. Iezekiel, "Self-oscillating optical frequency comb: Application to low phase noise millimeter wave generation and radio-over-fiber link," *J. Lightw. Technol.*, vol. 36, no. 19, pp. 4535–4542, Oct. 2018.

[19] K. Mallick *et al.*, "Bidirectional OFDM-MMWOF transport system based on mixed QAM modulation format using dual mode colorless laser diode and RSOA for next generation 5-G based network," *Opt. Fiber Technol.*, vol. 64, Jul. 2021, Art. no. 102562.

[20] C. -T. Tsai *et al.*, "Incoherent laser heterodyned long-reach 60-GHz MMWoF link with volterra filtered 16-QAM OFDM beyond 13 Gbps," *IEEE J. Sel. Topics Quantum Electron.*, vol. 27, no. 2, pp. 1–11, Mar./Apr. 2021.

[21] H. -Y Wang, C. -H. Cheng, C. -T. Tsai, Y. -C. Chi, and G. -R. Lin, "28 GHz wireless carrier heterodyned from orthogonally polarized tri-color laser diode for fading-free long-reach MMWoF," *J. Lightw. Technol.*, vol. 37, no. 13, pp. 3388–3400, Jul. 2019.

[22] C. -T. Tsai, C. -C. Li, C. -H. Lin, C. -T. Lin, S. Chi, and G. R. Lin, "Long-reach 60-GHz MMWoF link with free-running laser diodes beating," *Sci. Rep.*, vol. 8, Sep. 2018, Art. no. 13711.

[23] G. Carpintero *et al.*, "Microwave photonic integrated circuits for millimeter-wave wireless communications," *J. Light. Technol.*, vol. 32, no. 20, pp. 3495–3501, Oct. 2014.

[24] S. E. Alavi, M. R. K. Soltanian, I. S. Amiri, M. Khalily, A. S. M. Supa'at, and H. Ahmad, "Towards 5G: A photonic based millimeter wave signal generation for applying in 5G access fronthaul," *Sci. Rep.*, vol. 6, no. 1, Jan. 2016, Art. no. 19891.

[25] L. Fan, G. Xia, J. Chen, X. Tang, Q. Liang, and Z. Wu, "High-purity 60 GHz band millimeter-wave generation based on optically injected semiconductor laser under subharmonic microwave modulation," *Opt. Exp.*, vol. 24, no. 16, pp. 18252–18265, Aug. 2016.

[26] G.-W. Lu *et al.*, "Flexible generation of 28 Gbps PAM4 60 GHz/80 GHz radio over fiber signal by injection locking of direct multilevel modulated laser to spacing-tunable two-tone light," *Opt. Exp.*, vol. 26. no. 16, pp. 20603–20613, Aug. 2018.

[27] K. Balakier, M. J. Fice, L. Ponnampalam, A. J. Seeds, and C. C. Renaud, "Monolithically integrated optical phase lock loop for microwave photonics," *J. Lightw. Technol.*, vol. 32, no. 20, pp. 3893–3900, Oct. 2014.

[28] L. A. Johansson and A. J. Seeds, "Generation and transmission of millimeter-wave data-modulated optical signals using an optical injection phase-lock loop," *J. Lightw. Technol.*, vol. 21, no. 2, pp. 511–520, Feb. 2003.

[29] K. Zeb *et al.*, "InAs/InP quantum dash buried heterostructure mode-locked laser for high capacity fiber-wireless integrated 5G new radio fronthaul systems," *Opt. Exp.*, vol. 29, no. 11, pp. 16164–16174, May. 2021.

[30] A. Delmade *et al.*, "Quantum dash passively mode locked laser for optical heterodyne millimeter-wave analog radio-over-fiber fronthaul systems," in *Proc. Opt. Fiber Commun. Conf.*, 2020, Paper W2A.41.

[31] Q. Tareq, M. Ragheb, E. Alkhazraji, M. A. Esmail, S. Alshebeili, and M. Z. M. Khan, "Hybrid 28 GHz MMW over fiber-wireless QPSK transmission system based on mid L-band external injection-locked quantum-dash laser comb source," *Opt. Fiber Technol.*, vol. 64, Jul. 2021, Art. no. 102553.

[32] M. Z. M. Khan, Q. Tareq, A. M. Ragheb, M. A. Esmail, and S. A. Alshebeili, "Bidirectional MMWoF-wireless convergence system based on a 1610 nm L-band quantum-dash laser," *Opt. Exp.*, vol. 29, no. 17, pp. 27493–27507, 2021.

[33] M. Rahim *et al.*, "Monolithic InAs/InP quantum dash dual-wavelength DFB laser with ultra-low noise common cavity modes for millimeter-wave applications," *Opt. Exp.*, vol. 27, no. 24, pp. 35368–35375, Nov. 2019.

[34] K. Mallick, P. Mandal, R. Mukherjee, G. C. Mandal, B. Das, and A. S. Patra, "Generation of 40 GHz/80 GHz OFDM based MMW source and the OFDM-FSO transport system based on special fine tracking technology," *Opt. Fiber Technol.*, vol. 54, Jan. 2020, Art. no. 102130.

[35] G. C. Mandal, R. Mukherjee, B. Das, and A. S. Patra, "A full-duplex WDM hybrid fiber-wired/fiber wireless/fiberVLC/fiber-IVLC transmission system based on a self-injection locked quantum dash laser and a RSOA," *Opt. Commun.*, vol. 427, pp. 202–208, Nov. 2018.

[36] A. Ragheb, Q. Tareq, E. Alkhazraji, M. A. Esmail, S. Alshebeili, and M. Z. M. Khan, "Extended L-band InAs/InP quantum-dash laser in tunable millimeter-wave applications," *Photonics*, vol. 8, no. 5, May. 2021, Art. no. 167.

[37] H. Zhang *et al.*, "Quantum dot coherent comb laser source for converged optical-wireless access networks," *IEEE Photon. J*, vol. 13, no. 3, pp. 1–9, May 2021.

[38] M. J. Fice *et al.*, "146-GHz millimeter-wave radio-over-fiber photonic wireless transmission system," *Opt. Exp.*, vol. 20, no. 2, pp. 1769–1774, Jan. 2012.

[39] P. Mandal, K. Mallick, S. Santra, B. Kuiri, B. Dutta, and A. S. Patra, "A bidirectional hybrid WDM-OFDM network for multiservice communication employing self-injection locked qdash laser source based on elimination of rayleigh backscattering noise technique," *Opt. Quantum Electron.*, vol. 53, no. 5, Apr. 2021, Art. no. 263.

[40] P. Mandal *et al.*, "Hybrid WDM-FSO-PON with integrated SMF/FSO link for transportation of Rayleigh backscattering noise mitigated wired/wireless information in long-reach," *Opt. Commun.*, vol. 507, Mar. 2022, Art. no. 127594, doi: 10.1016/j.optcom.2021.127594.

[41] K. Mallick *et al.*, "Bidirectional OFDM based MMW/THzW over fiber system for next generation communication," *IEEE Photon. J.*, vol. 13, no. 4, pp. 1–7, Aug. 2021.

[42] Z. G. Lu *et al.*, "InAs/InP quantum dash semiconductor coherent comb lasers and their applications in optical networks," *J. Lightw. Technol.*, vol. 39, no. 12, pp. 3751–3760, Jun. 2021.

[43] R. Rosales *et al.*, "High performance mode locking characteristics of single section quantum dash lasers," *Opt. Exp.*, vol. 20, no. 8, pp. 8649–8657, Apr. 2012.

[44] F. Lelarge *et al.*, "Recent advances on InAs/InP quantum dash based semiconductor lasers and optical amplifiers operating at 1.55 um," *IEEE J. Sel. Topics Quantum Electron.*, vol. 13, no. 1, pp. 111–124, Feb. 2007.

[45] Z. G. Lu, J. Liu, P. J. Poole, C. Song, and S. Chang, "Ultra-narrow linewidth quantum dot coherent comb lasers with self-injection feedback locking," *Opt. Exp.*, vol. 26, no. 9, pp. 11909–11914, Apr. 2018.

[46] K. Merghem, V. Panapakkam, Q. Gaimard, F. Lelarge, and A. Ramdane, "Narrow linewidth frequency comb source based on self-injected quantum-dash passively mode-locked laser," in *Proc. Lasers Electro-Opt.*, 2017, Paper SW1C.5.

[47] P. J. Poole, K. Kaminska, P. J. Barrios, Z. G. Lu, and J. R. Liu, "Growth of InAs/InP-based quantum dots for 1.55 μm laser applications," *J. Cryst. Growth*, vol. 311, no. 6, pp. 1482–1486, Mar. 2009.

[48] R. A. Shafik, M. S. Rahman, and A. H. M. R. Islam, "On the extended relationships among EVM, BER and SNR as performance metrics," in *Proc. Int. Conf. Elect. Comput. Eng.*, 2006, pp. 408–411.

Khan Zeb received the B.Sc. degree in telecommunication engineering from the University of Engineering and Technology, Peshawar, Pakistan, in 2010, and the M.Sc. degree in electrical engineering from King Saud University, Riyadh, Saudi Arabia, in 2015. He is currently working toward the Ph.D. degree in electrical and computer engineering with Concordia University, Montreal, QC, Canada. From 2010 to 2011, he was a Transmission Network Engineer with LCC Pakistan Pvt. Ltd., Islamabad, Pakistan. From 2011 to 2014, he was a Research Assistant with the Department of Electrical Engineering, College of Engineering, King Saud University. From 2015 to 2016, he was a Researcher with the Center of Excellence in Information Assurance, King Saud University. Since September 2018, he has been a Visiting Ph.D. with Advanced Electronics and Photonics Research Centre, National Research Council, Ottawa, ON, Canada, where he is currently working on HTSN project. His research interests include radio-over-fiber, microwave photonics, 5G/6G fronthaul transmission systems, millimeter-wave and Terahertz photonics, optical space division multiplexing, optical communications, quantum-dot/dash (QD) semiconductor multiwavelength and coherent comb lasers, network traffic analysis, anomaly detection, and network security.

Zhenguo Lu (Member, IEEE) received the Ph.D. degree in 1992. He is currently a Principal Research Officer, Team Lead of Photonics and Project Leader of National Challenge Program HTSN in Advanced Electronics and Photonics Research Centre, National Research Council, Ottawa, ON, Canada. He is also an Adjunct Professor with the Department of Electrical and Computer Engineering, University of Ottawa, Ottawa, ON, Canada, and has been with Concordia University, Montreal, QC, Canada, since 2006. After the Ph.D., he was the recipient of the Alexander von Humboldt (AvH) Research Fellowship to work with the Institute of Semiconductor Electronics, RWTH Aachen, Germany, from 1993 to 1995. Then, he was with the Terahertz Research Centre of Rensselaer Polytechnic Institute, NY, USA, for two years. In 1997, he came to NRC as a Research Officer. From 2000 to 2002, he was the Director of R&D of BTI Systems Inc., Ottawa, ON, Canada. He has re-joined NRC as a Senior Research Officer. He is an expert in the field of photonics devices and system applications. He has more than 250 publications in the refereed journals and conference papers, and eight U.S. patents. He is a Fellow of the Optica.

Jiaren Liu was born in Sichuan, China, in 1963. He received the B.S. and M.S. degrees in physics from the University of Sichuan, Chengdu, China, in 1983 and 1989, respectively, and the Ph.D. degree in optics from the Nanjing University of Science and Technology, Nanjing, China, in 1992. He was a Teaching Assistant with the Department of Physics, University of Sichuan from 1983 to 1987, an Associate Research Scientist with the Shanghai Institute of Optics and Fine Mechanics, Shanghai, China, from 1992 to1996, a Postdoctoral Research Associate with Texas A&M University, College Station, TX, USA, and University of Toronto, Toronto, ON, Canada, from 1996 to 1999, and a Product Design Engineer and Manager from 1999 to 2001. Since 2001, he has been a Senior Research Officer with National Research Council Canada. He is the author of more than 150 peer reviewed articles and several patents. His research interests include quantum dot semiconductor lasers, fiber lasers, femtosecond laser micromachining, photonic devices, laser spectroscopy, quantum optics, and information optics.

Youxin Mao received the B.S. degree in physics and the M.S. degree in electronics science from Nankai University, Tianjin, China, in 1982 and 1985, respectively, and the Ph.D. degree in opto-electronics from Lancaster University, Bailrigg, U.K., in 1995. From 1985 to 1992, she was a Lecturer with the Department of Electronic Engineer, Tianjin University, Tianjin, China. From 1995 to 1997 and 1997 to 1999, she was a Research Associate with Lancaster University, and a NSERC Visiting Fellowship with National Research Council in Canada, respectively. She was a Research Scientist with Exploratory R&D Group, JDS Uniphase from1999 to 2003 and with Medical Biophysics, University of Toronto, Toronto, ON, Canada, from 2003 to 2006. Since 2006, she has been a Senior Research Officer with National Research Council Canada. She is the author of more than 150 peer reviewed articles. Her research interests include ultra-low timing jitter quantum-dot mode-locked semiconductor lasers, PAM and QAM data format digital coherent optical and wireless networks, high speed and high power wavelength swept laser, semiconductor laser package, fiber optics, ultra-small optical fiber probes, and optical coherence tomography.

Guocheng Liu received the Ph.D. degree in electrical and computer engineering from the University of Waterloo, Waterloo, ON, Canada, in 2015. From 2016 to 2017, he was a Postdoctoral Fellow with the University of Waterloo. From 2017 to 2019, he was an Optical Device Scientist with VueReal Inc. Since 2019, he has been a Research Associate with National Research Council Canada. His research interests include quantum dot semiconductor laser, ultrahigh-speed PAM, and QAM coherent optical networks.

Philip J. Poole received the B.Sc. degree in physics and the Ph.D. degree in solid state physics from Imperial College, University of London, London, U.K., in 1989 and 1993, respectively. Since 1993, he has been with National Research Council Canada, in the areas of semiconductor optics and crystal growth. His work has covered many areas of III-V semiconductor research, including optical spectroscopy, quantum well intermixing, and 24 years of experience in CBE growth of III-V compounds. His research interests include epitaxial growth of InP-based quantum dot structures for optoelectronic devices that can take advantage of the novel properties of quantum dots, such as multiwavelength and femtosecond mode-locked lasers. The use of selective area epitaxy to control the nucleation site of individual quantum dots for quantum information purposes is also studied. In particular the growth of InP nanowires containing InAs dots with the demonstration of non-classical optical properties, such as photon antibunching and entanglement.

Mohamed Rahim received the Diploma degree in physics from the University of Science and Technology Houari Boumediene, Algeria, in 1999, the M.Sc. degree in engineering physics from the Technical University of Munich, Munich, Germany, in 2005, and the Ph.D. degree in physics from the Swiss Federal Institute of Technology (ETH Zurich), Switzerland, in 2010. After a year as a Postdoctoral with ETH Zurich, optimizing the performances of mid-infrared VECSEL, he joined UQAM University (université du Québec à Montréal) for a Postdoctoral Fellowship during 2012–2014. In 2014, he joined the National Research Council Canada, as a Research Officer assigned to Photonic Group. His research interests include laser design, quantum dot lasers, photonics, and hybrid integrations.

Grzegorz Pakulski received the M.Sc. and Ph.D. degrees in physics from Adam Mickiewicz University, Poznan, Poland, in 1975 and 1983, respectively. During his work with the Academy of Technology in Bydgoszcz, Poland, he studied light scattering, ultrashort optical pulse generation, and phase transitions in ferroelectric and ferroelastic crystals. Since 1988, he has been continued his work with the University of Windsor, Windsor, ON, Canada, and the University of Toronto, Toronto, ON, Canada. In 1990, he joined Bel Northern Research/Nortel, where he investigated and designed high speed semiconductor distributed feedback lasers. Since 2003, he has been with National Research Council Canada, conducting research in areas of quantum well and quantum dot semiconductor lasers and amplifiers.

Pedro Barrios received the B.Sc. degree in electronic engineering from the IUPFAN, Maracay, Venezuela, in 1989, and the M.S. and Ph.D. degrees in electrical engineering from the University of Pittsburgh, Pittsburgh, PA, USA, in 1993 and 1997, respectively. He was a Postdoc with the NanoFAB Center, Texas A\&M University, College Station, TX, USA, during 1998–1999 and with the Department of Electrical Engineering, University of Notre Dame, Notre Dame, IN, USA, from 1999 to 2000. He is currently with the Advanced Technology Fabrication Group, Advanced Electronics and Photonics Research Centre, National Research Council of Canada, Ottawa, ON, Canada. He is also pursuing research in fabrication of electronic and optoelectronic devices on Si and III-Vs semiconductors. He has also investigated the oxidation of III-V native oxides (AlGaAs and InAlP) with focus in materials, fabrication and characterization of MOS and HEMT devices, and underwent research in electronic materials characterization and development of thin films and nanostructure devices on Si.

Martin Vachon received the B.Sc. and M.S. degrees in physics from the University of Ottawa, Ottawa, ON, Canada, in 2005 and 2008, respectively. Since 2008, he has been a Technical Officer with the National Research Council of Canada, Ottawa, ON, Canada. He is currently performs characterization measurements of photonic devices with Advanced Electronics and Photonics Research Centre.

Daniel Poitras received the Ph.D. degree in physics engineering from Ecole Polytechnique, Montreal, QC, Canada, in 2000, with focus on plasma deposited inhomogeneous optical films and coatings. He is currently a Senior Researcher with the National Research Council of Canada, Ottawa, ON, Canada. His main research interests include the application, design, fabrication, and characterization of optical coatings, including optical coatings on waveguide facets.

Weihong Jiang received the Ph.D. degree from the Institute of Semiconductors, Chinese Academy of Sciences, Beijing, China, in 2000. From 2000 to 2005, she was a Postdoc, then a Research Associate, and later a Research Engineer with the Centre for Electrophotonic Materials and Devices (now the Center for Emerging Device Technologies), McMaster University, Hamilton, ON, Canada. In 2005, she joined the National Research Council Canada, Ottawa, ON, Canada. She is currently a Research Officer with the Advanced Electronics and Photonics Research Centre of NRC, working on Si and III-V based quantum well and quantum dots optoelectronic devices.

John Weber received the Bachelors of Mechanical Engineering from Carleton University, Ottawa, ON, Canada, in 1991. He had previously been with JDS Uniphase (now Lumentum and Viavi), Nortel Networks and Scintrex Trace in the development of a variety of electronic and fiber-optic components, test instrumentation, and sub-systems before joining the National Research Council in 2009. As part of the System Integration and Prototyping team, he was with researchers to develop experimental and prototype package designs for novel electronic and photonic devices.

Xiupu Zhang (Senior Member, IEEE) received the B.Sc. degree in electrical engineering from the Harbin Institute of Electrical Technology (now Harbin University of Science and Technology), Harbin, China, in 1983, the M.Sc. degree in electrical engineering from the Beijing University of Posts and Telecommunications, Beijing, China, in 1988, and the Ph.D. degree in electrical engineering from the Technical University of Denmark, Lyngby, Denmark, in 1996. From 1983 to 1985, he worked for manufacturing fibers and fiber cables in China. From 1985 to 1988, he studied for the master's degree with the Beijing University of Posts and Telecommunications. From 1988 to 1992, he was engaged in the construction of telecommunication networks in Beijing, China. From 1992 to 1996, he studied for the Ph.D. degree with the Technical University of Denmark. He then spent approximately one and a half years with the Chalmers University of Technology, Göteborg, Sweden, where he investigated high-speed fiber-optic transmission. From 1998 to 2002, he was a Senior Engineer with Fiber-Optics Industry, involved in the design of repeaterless fiber-optic transmission systems, design of erbium-doped fiber amplifiers and fiber Raman amplifiers, design of optical transmitters and receivers, and design of metropolitan optical networks, in North America, including Montreal and Ottawa, Canada, and Piscataway, NJ, USA. In June 2002, he joined Concordia University, Montreal, QC, Canada, and became an Associate Professor. He is currently a Full Professor with the Department of Electrical and Computer Engineering, Concordia University. He has authored or coauthored about 140 journal publications published in IEEE, Optical Society of America, and other related journals. His current research interests include 5G/6G fronthaul transmission systems, quantum-dot semiconductor lasers, broadband and high-power photodiodes, mode division multiplexed fiber optic transmission, and microwave/millimeter-wave circuits for 5G/6G.

Jianping Yao (Fellow, IEEE) received the Ph.D. degree in electrical engineering from the Université de Toulon et du Var, Toulon, France, in December 1997. He is currently a Distinguished University Professor and the University Research Chair with the School of Electrical Engineering and Computer Science, University of Ottawa, Ottawa, ON, Canada. From 1998 to 2001, he was with the School of Electrical and Electronic Engineering, Nanyang Technological University, Singapore, as an Assistant Professor. In December 2001, he was an Assistant Professor with the School of Electrical Engineering and Computer Science, University of Ottawa, where he was promoted to an Associate Professor in May 2003, and a Full Professor in May 2006. In 2007, he was appointed the University Research Chair in Microwave Photonics. In June 2016, he was conferred the title of Distinguished University Professor of the University of Ottawa. From July 2007 to June 2010 and July 2013 to June 2016, he was the Director of the Ottawa-Carleton Institute for Electrical and Computer Engineering. He has authored or coauthored more than 650 research papers, including more than 380 papers in peer-reviewed journals and more than 270 papers in conference proceedings. He is the Editor-in-Chief of the IEEE PHOTONICS TECHNOLOGY LETTERS, the former Topical Editor of the *Optics Letters*, and a former Associate Editor for the *Science Bulletin*. He is an Advisory Editorial Board Member of the *Optics Communications* and was a Steering Committee Member of the *Journal of Lightwave Technology* from 2017 to 2021. He was the Guest Editor of a Focus Issue on Microwave Photonics in *Optics Express* in 2013, Lead-Editor of a Feature Issue on Microwave Photonics in *Photonics Research* in 2014, and Guest Editor of a special issue on Microwave Photonics in IEEE/OSA JOURNAL OF LIGHTWAVE TECHNOLOGY in 2018. He was the Technical Committee Chair of IEEE MTT-S Microwave Photonics from 2017 to 2021 and an Elected Member of the Board of Governors of the IEEE Photonics Society during 2019– 2021. He was a Member of European Research Council Consolidator Grant Panel in 2016, 2018, and 2020, a Member of the Qualitative Evaluation Panel in 2017, and a panelist of the National Science Foundation Career Awards Panel in 2016. He was also the Chair of a number of international conferences, symposia, and workshops, including the Vice Technical Program Committee (TPC) Chair of the 2007 International Topical Meeting on Microwave Photonics, TPC Co-Chair of the 2009 and 2010 Asia-Pacific Microwave Photonics Conference, TPC Chair of the high-speed and broadband wireless technologies subcommittee of the IEEE Radio Wireless Symposium 2009–2012, TPC Chair of the microwave photonics subcommittee of the IEEE Photonics Society Annual Meeting 2009, TPC Chair of the 2010 International Topical Meeting on Microwave Photonics, General Co-Chair of the 2011 International Topical Meeting on Microwave Photonics, TPC Co-Chair of the 2014 International Topical Meetings on Microwave Photonics, General Co-Chair of the 2015 and 2017 International Topical Meeting on Microwave Photonics, and General Chair of the 2019 International Topical Meeting on Microwave Photonics. He was also a Committee Member for a number of international conferences, such as IPC, OFC, CLEO, BGPP, and MWP. He was the recipient of the 2005 International Creative Research Award of the University of Ottawa, 2007 George S. Glinski Award for Excellence in Research, in 2008, he was awarded the Natural Sciences and Engineering Research Council of Canada Discovery Accelerator Supplements Award, 2017–2018 Award for Excellence in Research of the University of Ottawa, and 2018 R.A. Fessenden Silver Medal from IEEE Canada. He was selected to receive an inaugural OSA Outstanding Reviewer Award in 2012 and was one of the top ten reviewers of the *Journal of Lightwave Technology* 2015–2016. He was the IEEE MTT-S Distinguished Microwave Lecturer 2013–2015. He is a Registered Professional Engineer of Ontario. He is a Fellow of the Optica, Canadian Academy of Engineering, and Royal Society of Canada.